I. INTRODUCTION

There is great interest in the study of epitaxial growth of metals on single crystal substrates.[1,2,3,4,5] This scientific problem is of considerable importance, both for experimental and theoretical reasons. The surface structure determines the reactivity and selectivity of bimetallic catalysts.[6] New compounds can be produced which show new and different properties of the commonly observed metal structures. There are a substantial number of publications dealing with the theoretical[7,8] and experimental properties of metallic overlayers.[1-5] A great diversity of techniques has been employed to investigate the electronic properties of metallic overlayers.[1-5,9] Recently, LEED measurements have been performed of Ni grown on Cu(111),[4] of Cu on Ni(100)[5] and Ni on Cu(100).[10] LEED is perhaps the most fundamental technique for characterization of the surface structure of epitaxially grown metal overlayers. A complete dynamical analysis of LEED intensity versus energy curves permits the determination of the interlayer spacing of epitaxially grown metal overlayers.[4,5,10] The employment of this technique is of great importance specifically for the determination of lattice parameters for structures like fcc iron epitaxially grown of Cu(100).[11,12] The ability to prepare fcc iron films by epitaxial growth on copper single crystals has been successfully demonstrated.[11,12,13,14] In the present work we report a sytematic LEED study of iron fcc grown on Cu(100), a full dynamical analysis was performed using the renormalized forward scattering perturbation method.

From the temperature dependence of the intensity versus energy (I-E)

curves of the (00) beam, we were able to determine the Debye temperatures for 1 ML and 10 Layers of fcc iron.

II. EXPERIMENTAL TECHNIQUES

The metal deposition and measurements were performed in an ultra-high vacuum chamber, which it has been previously described.[3,5,10] Prior to each Fe evaporation, the Cu(100) crystal was cleaned by several cycles of Ar ion sputtering and subsequent annealing at 550°C for 10 minutes. An occasional oxygen treatment was used to remove all impurities from the copper. The iron metal was evaporated from a Knudsen cell, consisting of an alumina crucible inserted inside a tantalum furnace. A shutter in front of the Knudsen cell allowed outgassing and stabilization of the deposition rate to facilitate reproducibility in the evaporation of the metal. Samples were prepared with the substrate at 190°C and at room temperature (RT). All the LEED measurements were performed at RT. The results reported here were performed with the substrate at RT during deposition. The LEED spots were very well defined and clear, although the samples deposited at 190°C showed even sharper spots. We observed that at 190°C over a long period of time (about 1 hr), there is clear evidence of surface seggregation of copper, because of this we decided to use the measurement for samples deposited at RT.

Auger electron spectroscopy (AES) was used to monitor the Fe thickness and purity. A Varian single-pass cylindrical mirror analyzer (CMA) with a coaxial electron gun was used in normal incidence for the AES measurements. The variation in intensity of the 651 eV iron Auger peak and the 920 eV

copper peak was used to determine the coverage.[11] For low iron coverage, better sensitivity is obtained by monitoring the attenuation of the $M_{2,3}VV$ and M_1 VV Auger transition of copper as a function of iron deposition. The Auger measurements suggest that iron growth approximately layer-by-layer on Cu(100).

The LEED pattern persisted with sharp spots up to about 17 layers of iron on Cu(100). However, at such high coverages, there is evidence of oxygen and carbon impurities[11] (less than 0.1 of a ML). In the present measurements, we report LEED results for 1 ML and 10 layers of iron. The latter is taken as representative of bulk fcc iron at room temperatures.

LEED intensity-versus-energy curves were obtained by using a spot photometer (Photo Research, Model UBD-1/4). The output voltages from the spot photometer and the beam current from the LEED module were passed through an ADC into and Apple II+ computer. A Varian four-grid LEED system was used in these measurements. Prior to the measurements, adjustments using trimming magnets, Helmhotz coils and θ-and ϕ-rotations were made so that all spots of the same symmetry had equal intensities. Energy scales are given with reference to the vacuum level. The experimental intensity versus energy spectra were recorded for (10), (01), (10), (01), (11), (11), (11), (11), (20), (20), (02), (02), and (00). The symmetry related beams were averaged to correct for any small misalignment. In order to obtain the I vs E curves for the (00) beam, the sample was tilted out of the axis of the electron gun. The value of the angles θ and ϕ could be measured directly from the photographs of the LEED pattern. In this work we employed the method described by Cunningham and Weinberg[15] to determine θ and ϕ.

III. RESULTS AND DISCUSSION

Our theoretical calculations for the Fe/Cu(100) system were based on the dynamical theory of LEED.[16]. Our program is based on the computer programs developed by Van Hove and Tong.[17] In these calculations, surface and layer potentials have muffin-tin geometry; i.e., the potential consists of an array of spherically symmetric non overlapping potentials embedded in a constant background potential. The crystal is divided into layers of identical 2-D symmetry, each layer consisting of a single bravais lattice. Diffraction from each layer is calculated exactly, reflection and transmission by stacked layers are evaluated by the renormalized forward scattering method.[16] The temperature effect is included through temperature dependent phase shifts using a Debye-Waller factor. Fifty-seven beams and eight phase shifts were used in our calculations. We vary in addition to the structural parameters (interlayer spacings), the non-structural parameters; internal potential and Debye temperature. The surface and substrate Debye temperatures were determined by comparing theoretical calculations with experimental data taken at four different temperatures 273, 373, 473 and 573 K for the (00) beam. We allowed the internal potential to vary as a function of incident beam energy. Correlation effects are less important at high energies, and the energy dependence of the internal potential approximately takes into account the decrease in the screening as the incident beam energy increases. We find that allowing the internal potential to be energy dependent makes little difference in our calculations for 10 layers of iron. Experimental spectra for the (00), (10), (11) and (20) beams were compared with theoretical curves for each geometry, and the quality of the agreement was judged using

the R = r (ΔE) factor defined by Legg et al.[18] This factor is the product of r, which compares relative peak heights, and (ΔE), which is a measure of peak displacement. Smaller values of R correspond to better agreement with the experimental values.[18,5,110]. In our calculations a multiple relaxation approach is used in analysing the experimental results (d_{12} first layer, d_{23} second layer and substrate are independently varied).

The LEED measurements were performed for one monolayer and ten layers of iron on Cu(100). Normal incidence was used for the (10), (11) and (20) beams. The energy range for the (00) beam was from 25 to 470 eV. The peak positions and intensities of the I-E curves vary as a function of iron coverage, but remain consistent with an fcc lattice of iron growing epitaxially on Cu(100). The (00) beam shows the greatest sensitivity to changes in the iron coverages. There is a small lattice mismatch between the lattice parameters for Cu fcc (3.61Å) and the expected lattice parameter for fcc Fe, (3.58Å).[11,12] One expects iron to be partially strained to obtain a perfect match and form the observed (1 x 1) patterns.

In order to find the best values for the structural and nonstructural parameters, we performed independent calculations where some parameters were fixed and the others varied until a minimum R was found. This procedure was repeated consistently until a minumum R value was obtained.

1 ML Fe on Cu(100):

We performed several independent calculations for one monolayer of Fe on Cu(100). We fixed the Debye temperature and internal potential (at a constant value of -11 eV) and varied the interlayer spacings. We then fixed the interlayer spacings (d23) and Debye temperature of Cu, and varied the

surface Debye temperature and d_{12}. We repeated the same procedures fixing the Debye temperatures and varying the interlayer spacings and using an energy dependent internal potential. This process was repeated until all the parameters were consistent with a minimum in R.

We also calculated the temperature dependence of the I-E curves for the (00) beam ($\theta = 4.8 \pm 0.2^{o}$, $\gamma = 29 \pm 1^{o}$) taken at four different temperatures 273, 373, 473, and 573 K (error of about 5 K). We determined the value of the Debye temperature to be 233 ± 10 K. In figure 1 the I-E curves are shown for four different temperatures, the calculated curves are given by the dotted lines. The bulk Cu Debye temperature (344 K) was used for the substrate. With the exception of the very low energy peaks, as the temperature increases, the intensity of the peaks decreases. The exception is the peak at 36.6 eV, shown in Figure 2. The intensity of that peak increases at 473 K. It is evident from these measurements that there is surface seggregation of Cu (or equivalent iron diffusion), this peak clearly belongs to the substrate. Such a phenomenon was independently corroborated using Auger spectroscopy.

The second iron structural parameter we determined was the internal potential. An initial set of calculations was performed and a value of -11 eV was obtained for the internal potential. We improved considerable the reliability factor value by allowing the internal potential to vary as a function of energy (we observed a 50% decrease in R). The energy dependence of the internal potential is shown in Figure 3. The effect of varying the internal potential is to give a uniform shift in the position of the peaks. As the internal potential decreases, the peak positions shift to lower energy values. The need for such a variation in the

internal potential is attributed to the importance of Fe/Cu interface for the monolayer coverage. Recent theoretical calculation of a monolayer of iron on Cu(100) have shown that considerable changes take place on the DOS for one monolayer of iron on Cu(100).[19]

In figure 4 we show a comparison of the experimental measurements for the (00), (10), (11) and (20) beams and the theoretical calculations for various interlayers spacings. The best agreement obtained from the reliability factor corresponds to a value of $d_{12} = 1.78 \pm 0.02$ Å and $d_{23} = 1.81 \pm 0.02$ Å (essentially bulk Cu(100)). Figure 5 shows the variation of the reliability factor as a function of d_{12} and d_{23} and Figure 6 shows the variation of the reliability factor as a function of the surface Debye temperature and d_{12}. All the peaks were included in the R value analysis, if only a limited number (only major peaks) are used the R value decreases even more.

10 Layers of Fe on Cu(100):

We consider that the sample containing 10 layers of iron epitaxially grown on Cu(100) corresponds to bulk fcc Fe. We employed the same procedures used for 1 ML Fe to analyze the 10 layers case. We varied both the structural and nonstructural parameters. However, in this case the number of variables is increased by one: the unknown Debye temperature of fcc Fe(100). The bulk Debye temperature of bcc Fe is well known (470 K), to find the bulk Debye temperature of fcc Fe we need to analyze the temperature dependence of the (00) beam. We varied the values Θ_D bulk between 350 and 600 K, and use the relation Θ_D (surface) = $\frac{\Theta_D}{\sqrt{2}}$ (bulk). The best agreement to the experimental data was obtained for bulk fcc Fe with a $\Theta_D = 550 \pm 10$ K and the corresponding surface temperature is 380 ± 10K. In

Figure 7 we plotted the I-E curves calculated with the best values of Θ_D for four different temperatures (dotted lines) and the experimental measurements (continuous line).

We varied the interlayer spacing for the surface d_{12}, substrate d_{23} and bulk. In Figure 8 we compare the theoretical calculations for various interlayer spacings with the experimental data for the (00), (10), (11) and (20) beams. The smallest value of the reliability factor (R = 0.06) corresponds to $d_{12} = 1.81 \pm 0.02$ Å and $d_{23} = 1.78 \pm 0.02$ Å (The same value also for the bulk). Using a value of 1.794 Å for bulk fcc, d_{12} and d_{23} we obtained R = 0.19. The results for this value are shown in the curve labelled C of Figure 8. When we contract the surface interlayer spacing and expand the substrate interlayer spacing, the reliability factor increases to 1.0 (see curve E). We also varied the 2-D lattice vectors, two independent multiple relaxation calculations were done first with an fcc lattice parameter of 3.58 Å and second with 3.61 Å. We found that values for the interlayer relaxation obtained in both cases were in good agreement with the ones reported in Table I. Figure 9 shows the variation of the reliability factor as a function of d_{12} and d_{23}. The internal potential that best fits the data is -11eV and doesn't show the energy dependence observed for one monolayer. This is taken as another evidence of the influence of the Fe-Cu interface, which is negligible for the 10 layers sample. In Table I we summarized the results of our analysis of the LEED measurements for 1 ML and 10 layers iron fcc on Cu(100). We observed a contraction of the interlayer spacing for 1 ML Fe on Cu(100) in agreement with other workers observations on elemental systems (20). For 10 layers the best agreement is obtained for a small expansion of the surface overlayer as compared to the bulk.

Our reliability factor for 1 ML Fe on Cu(100) is five times larger than the one obtained for 10 layers Fe on Cu(100). This may be related to our use of a superposition of atomic potentials to obtain the crystal potential, which neglects the re-arrangement of charge on the Fe/Cu interface. It is also noted that the high energy peaks are those which show the largest disagreement between the theoretical calculations and the experiment. Restricting the range of energies included in our calculations reduces the R values, but doesn't change the values obtained for the structural and nonstructural parameters.

IV. CONCLUSIONS

We have studied the growth of iron on Cu(100) and determined the structural and nonstructural parameters from a full LEED analysis of 1 ML and 10 layers of iron. From the temperature dependence of the (00) beam, the Debye temperature of fcc iron were also obtained.

V. ACCKNOWLEDGEMENTS

The authors acknowledge helpful discussion with B.R. Cooper, G.W. Fernando, Y.C. Lee, J.M. Wills and B.M. Davies. This work was supported by the U.S. Department of Energy.

VI. REFERENCES

1. A. Chambers and D.C. Jackson Phil. Mag. 31, 1357 (1975).
2. I. Abbate, L. Braicovich, and A. Fasan Phil. Mag. B44, 327 (1981).
3. P.A. Montano, P.P. Vaishnava, and E. Boling Surf. Sci. 130, 191 (1983).
4. S.P. Tear and K. Roll, J. Phys. C: Solid State Phys. 15, 5521 (1982).
5. M. Abu-Joudeh, P.P. Vaishnava and P.A. Montano, J. Phys. C. Solid State Phys. 17, 6899 (1984).
6. J.H. Sinfelt, Surf. Science 195, 641 (1977).
7. C.S. Wang and A.J. Freeman Phys. Rev. B19, 793 (1979).
8. C.Q. Ma, H. Krakauer and B.R. Cooper, J. Vac. Sci. Techn. 18, 581 (1981).
9. M.A. Thompson and J.L. Erskine, Phys. Rev. B31, 16832 (1985).
10. M.A. Abu-Joudeh, B.M. Davies, and P.A. Montano, Surface Science 1986 (in Press).
11. Y.C. Lee, H. Min and P.A. Montano, Surf. Science 166, 391 (1986).
12. P.A. Montano, Y.C. Lee, J. Marcano and H. Min, MRS Proceedings, Layered Structures and Epitaxy (1986).
13. U. Gradmann and P. Tillmanns, Phys. Stat. Sol. (1) 44, 539 (1977).
14. W. Wiartolla, W. Becker, W. Keune, and H.D. Pfannes, J. de Physique 45, C5-461 (1984).
15. S.L. Cunningham and W. Henry Weinberg, Rev. Sci. Instr. 49, 752 (1978).
16. J.B. Pendry, "Low Energy Electron Diffraction" London, New York, Academic Press (1974).

17. M.A. Van Hove and S.Y. Tong "Surface Crystallography by LEED," Berlin, Springer Verlag (1979).

18. K.O. Legg, F. Jona, D.W. Jepsen, and P.M. Marcus, J. Phys. C. 10, 937 (1977).

19. G.W. Fernando, Y.C. Lee, P.A. Montano, B.R. Cooper, E.R. Moog, H.M. Naik and S.D. Bader, (to be published).

20. H.L. Davis and J.R. Noonan, J. Vac. Sci. Techn. 20, 842 (1982) Surface Sci. 126, 245 (1983).

TABLE I

Interlayer spacings and Debye Temperatures for 1 ML Fe on Cu(100) and 10L Fe on Cu(100).

Fe on Cu(100)	d_{12} (Å)	d_{23} (Å)	d bulk	Surface Debye Temp. (K)	Substrate Debye Temp. (K)
1 ML	1.78±0.02	1.81±0.02	1.81±0.02	233± 10K	344± 10
10 L	1.81±0.02	1.78±0.02	1.78±0.02	380± 10K	550± 10

d_{12} = topmost interlayer spacing.

d_{23} = interlayer spacing between the second and third layers.

FIGURE CAPTIONS

Figure 1: I-E curves for the (00) beam of one monolayer Fe on Cu(100) at four different temperatures ($\theta = 4.8 \pm 0.2^{\circ}$ $\phi = 29 \pm 1^{\circ}$, Substrate Debye Temp. = 344° K Surface Debye Temp. = 233° K).

Figure 2: Experimental I-E curves for the (00) beam of one monolayer Fe on Cu(100) at four different temperatures. ($\theta = 4.8 \pm 0.2$, $\phi = 29 \pm 1$).

Figure 3: The energy dependence of the internal potential for one monolayer Fe on Cu(100).

Figure 4: I-E curves for the (00), (10), (11) and (20) beams of one monolayer of Fe on Cu(100): The top curves are experimental, curves A,B,C,D,E are theoretical calculations with different interlayer spacings. For the (00) beam ($\theta = 4.8 \pm 0.2$, $\phi = 29 \pm 1$).

(A) $d_{12} = 1.77$ Å, $d_{23} = 1.81$ Å,

(B) $d_{12} = 1.83$ Å, $d_{23} = 1.78$ Å,

(C) $d_{12} = 1.79$ Å $d_{23} = 1.79$ Å,

(D) $d_{12} = 1.77$ Å, $d_{23} = 1.82$ Å,

(E) $d_{12} = 1.69$ Å, $d_{23} = 1.83$ Å.

Figure 5: Three dimensional contour plot for 1 monolayer Fe on Cu(100). The variation of the reliability factor as a function of d_{12} and d_{23}.

Figure 6: Three dimensional contour plot for one monolayer Fe on Cu(100). The variation of the reliability factor as a function of surface Debye temperature and d_{12}.

Figure 7: I-E curves for the (00) beam of 10 layers of Fe on Cu(100) at four different temperatures. $\Theta = 5 \pm 0.2$, $\phi = 28 \pm 1$, Substrate Debye Temp = 550° K, Surface Debye Temp = 380° K.

Figure 8: I-E curves for the (00), (10), (11) and (20) beams of 10 layers of Fe Cu(100). The top curves are experimental. The curves A,B,C,D and E a theoretical curves with different interlayer spacings. For the (00) beam ($\Theta = 5 \pm 0.2$, $\phi = 28 \pm 1$).

(A) $d_{12} = 1.81\mathring{A}$, $d_{23} = 1.770\ \mathring{A}$

(B) $d_{12} = 1.794\mathring{A}$, $d_{23} = 1.780\mathring{A}$

(C) $d_{12} = 1.794\mathring{A}$, $d_{23} = 1.794\mathring{A}$

(D) $d_{12} = 1.81\ \mathring{A}$, $d_{23} = 1.75\mathring{A}$

(E) $d_{12} = 1.76\mathring{A}$, $d_{23} = 1.83\mathring{A}$

Figure 9: Three dimensional contour plot for 10 layers of Fe on Cu(100). The variation of the reliability factor as a function of d_{12} and d_{23}.

Fig 1

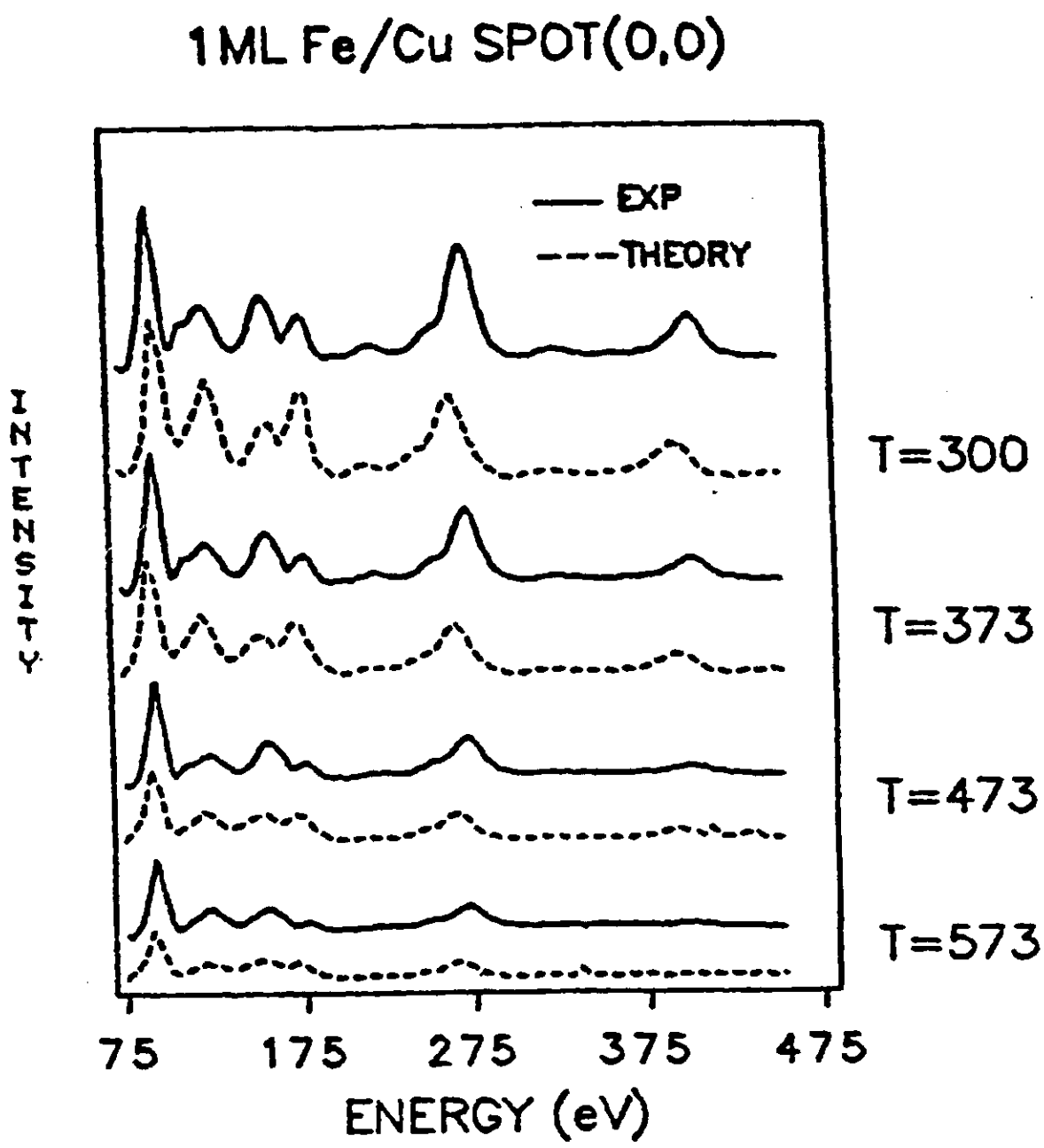
1ML Fe/Cu SPOT(0,0)
EXP
THEORY
T=300
T=373
T=473
T=573
INTENSITY
75
175
275
375
475
ENERGY (eV)

F;)2

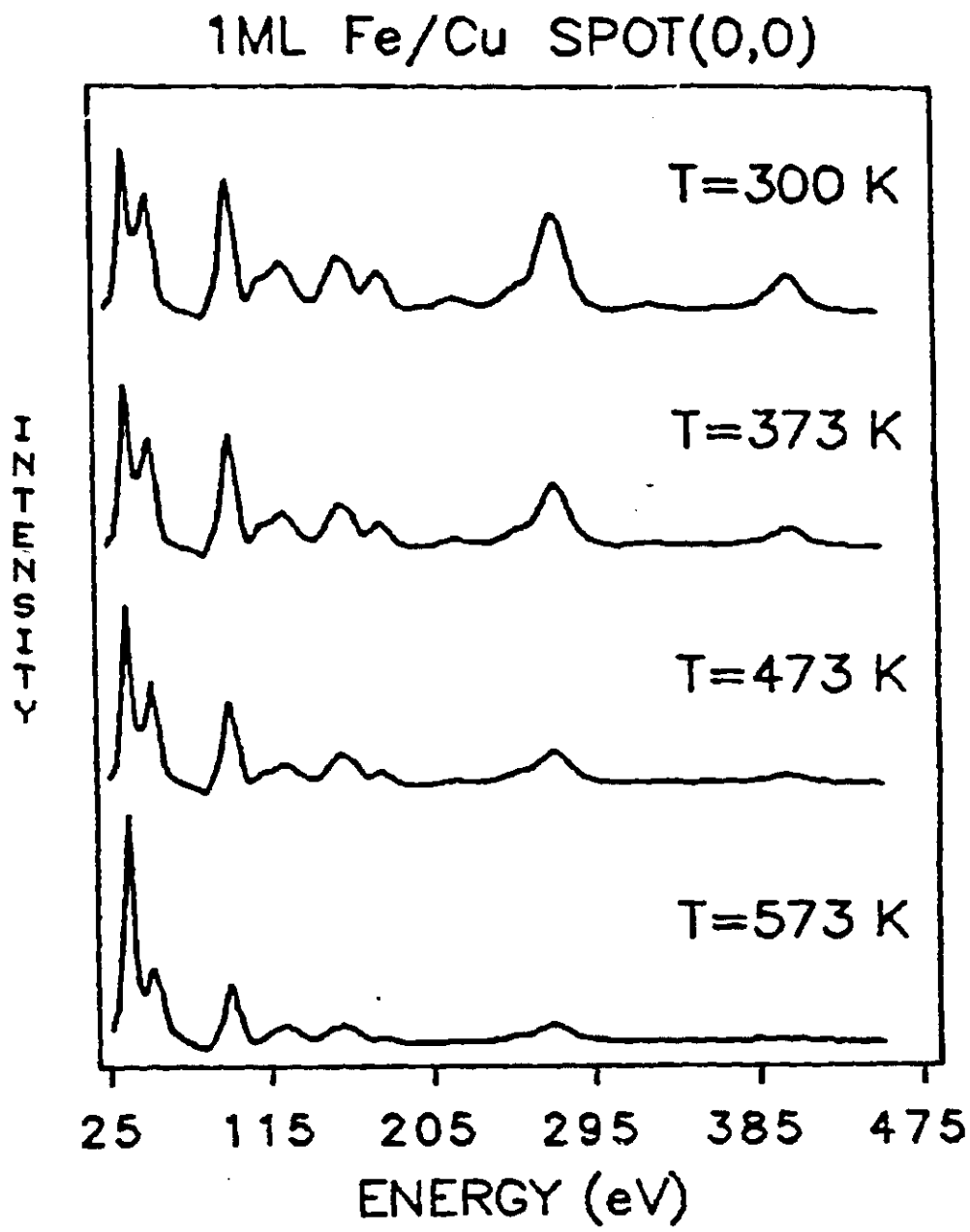
1ML Fe/Cu SPOT(0,0)
T=300 K
T=373 K
T=473 K
T=573 K
INTENSITY
25
115
205
295
385
475
ENERGY (eV)

Fig 3

1ML Fe/Cu (100)

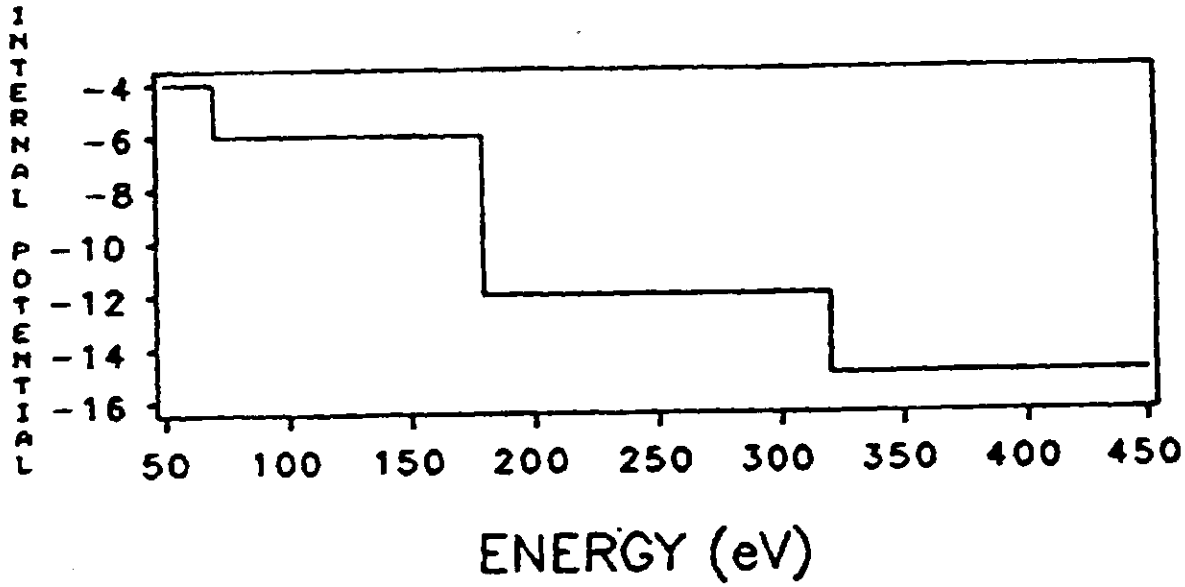

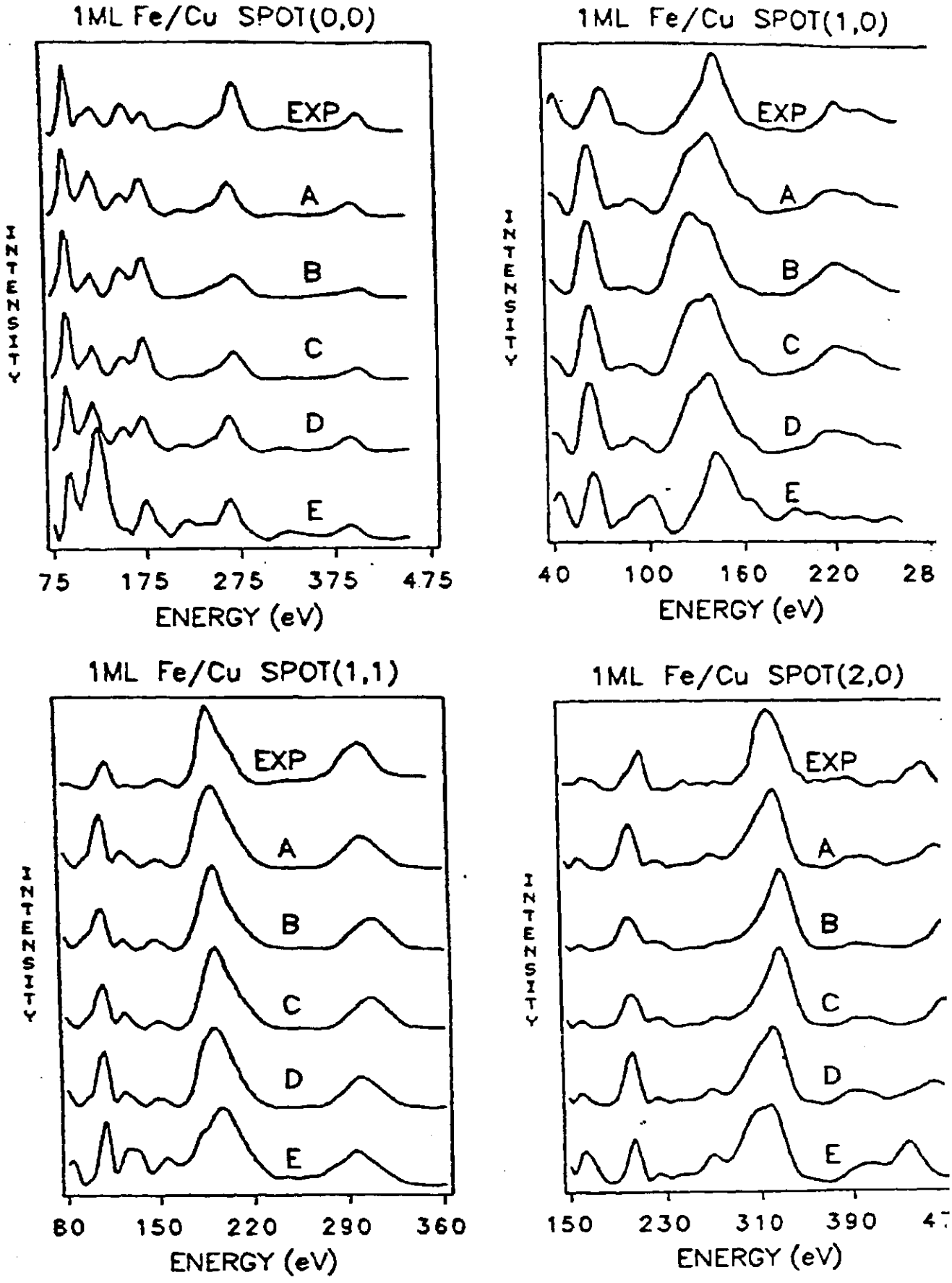
1ML Fe/Cu SPOT(0,0)
EXP
A
B
C
D
E
INTENSITY
75
175
275
375
475
ENERGY (eV)
1ML Fe/Cu SPOT(1,0)
EXP
A
B
C
D
E
INTENSITY
40
100
160
220
28
ENERGY (eV)
1ML Fe/Cu SPOT(1,1)
EXP
A
B
C
D
E
INTENSITY
80
150
220
290
360
ENERGY (eV)
1ML Fe/Cu SPOT(2,0)
EXP
A
B
C
D
E
INTENSITY
150
230
310
390
ENERGY (eV)

F.8 5

Reliability Factor

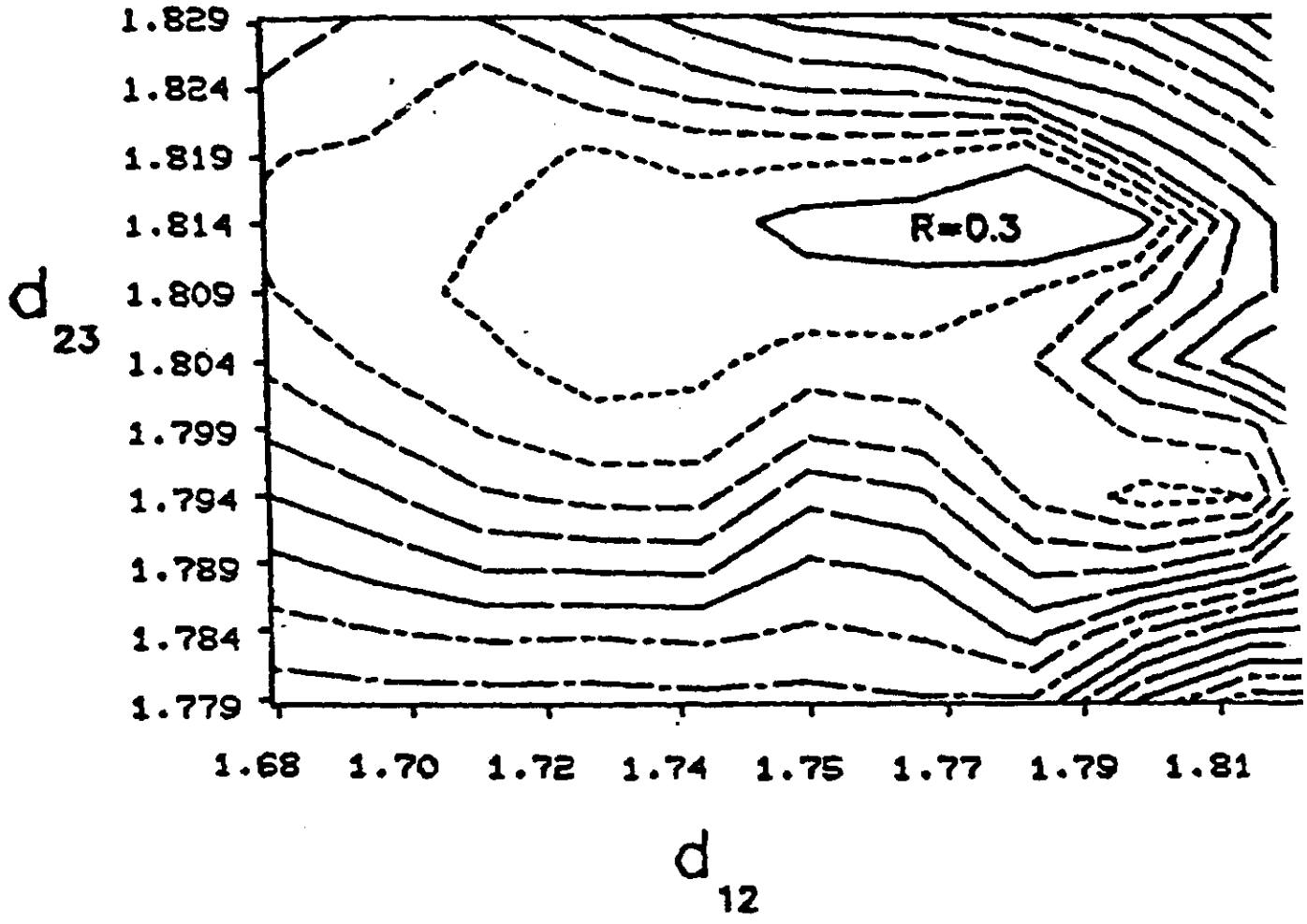

FIG 6

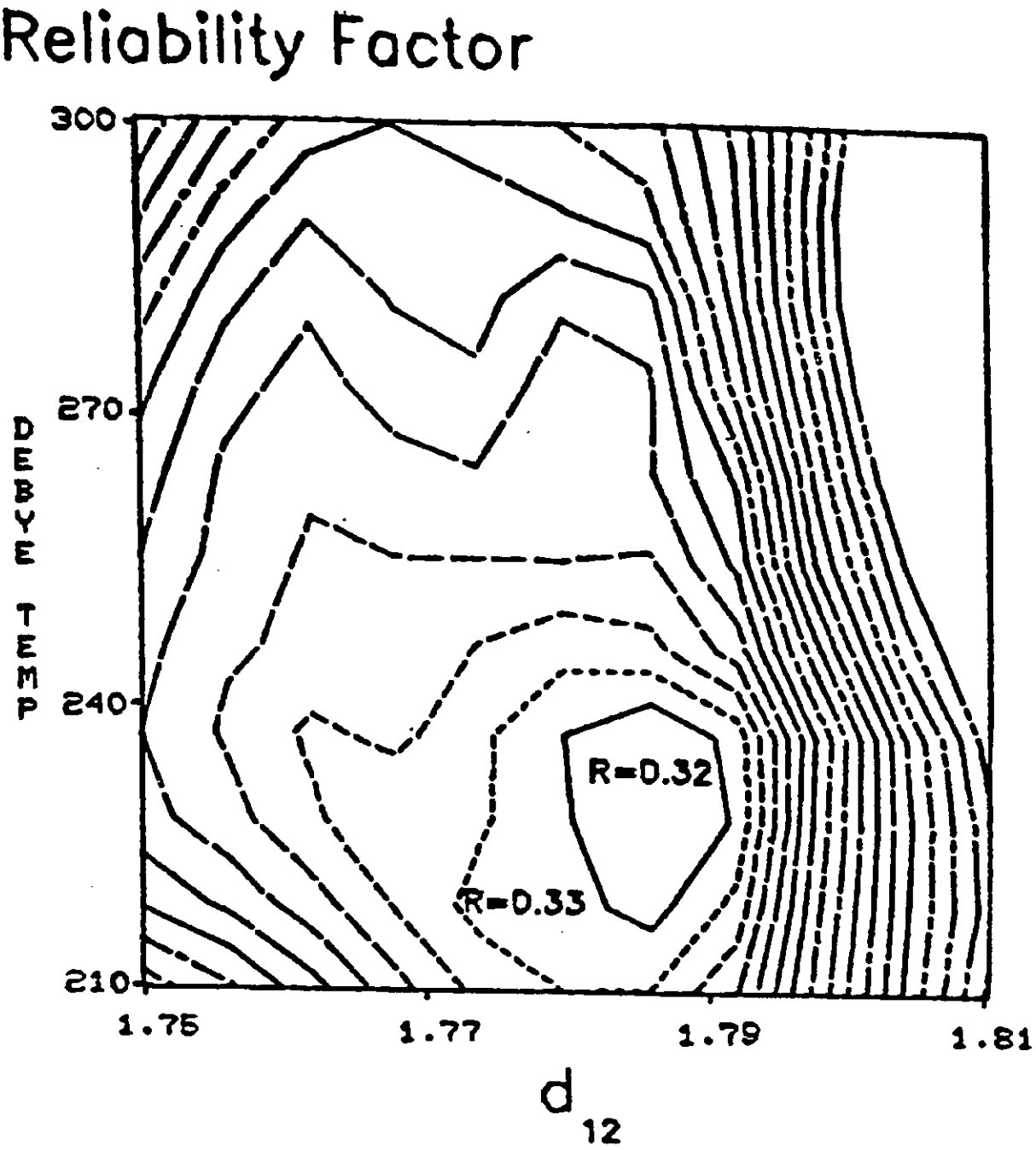
Reliability Factor
300
270
240
210
DEBYE TEMP
R=0.32
R=0.33
1.75
1.77
1.79
1.81
d12